Environmental Pollution 249 (2019) 225–235

Contents lists available at ScienceDirect

Environmental Pollution

journal homepage: www.elsevier.com/locate/envpol

Nutrient burial and environmental changes in the Yangtze Delta in response to recent river basin human activities☆

Yueying Liu, Bing Deng*, Jinzhou Du, Guosen Zhang, Lijun Hou

State Key Laboratory of Estuarine and Coastal Research, East China Normal University, Shanghai, 200241, China

ARTICLE INFO

Article history:
Received 26 November 2018
Received in revised form
5 March 2019
Accepted 10 March 2019
Available online 12 March 2019

Keywords:
Environmental changes
Sediment records
Nutrient burial
Human activities
Yangtze delta

ABSTRACT

High resolution sediment records in the Yangtze Delta front were constructed to reveal recent environmental changes in response to river basin human activities. Increases in nutrient and organic C influxes that began in the 1950s, together with elevated primary productivity and increased chemical fertilizer application, suggested a shift toward anthropogenic-predominated environmental changes during this period. The depletion of total organic C (TOC), total N (TN), and biogenic Si (BSi), along with the decline in sedimentation rate and coarsening of sediment coincided with the development of hydrological engineering in the river basin from the 1980s. Reservoir Si retention substantially altered river mouth primary productivity community composition from diatoms to non-diatoms, thereby changing the BSi/TOC molar ratio in the sediment profile. Estimation of biogenic component burial fluxes was conducted to assess the variation and potential impacts. A recent dramatic decline in biogenic component burial in the delta area suggested a low nutrient removal efficiency in this region, due to the decrease in sediment discharge. Consequently, more nutrients have been further transported to the inner shelf and open waters instead of being buried in the delta sediment, thereby increasing the environmental pressure in the Yangtze Delta and adjoining coastal area.

1. Introduction

Deltas are important interfaces between terrestrial and oceanic ecosystems in which land, rivers, estuaries, ocean, and the atmosphere interact (Bianchi and Allison, 2009; Walsh, 2013). Densely populated, and of ecological and economic importance, deltas are highly sensitive and vulnerable to global climate change and human activities (Bianchi and Allison, 2009; Syvitski et al., 2009; Giosan et al., 2014; Kong et al., 2015).

The Yangtze River, one of the largest turbid rivers in the world, covers a drainage area of approximately 1.8 million km^2. The river basin has a population of over 400 million, of which approximately 40% is concentrated in the river delta. The formation of habitats and ecosystems heavily relies on the service functions of the river system. However, during past decades, intensive human activities have substantially increased the discharge of agricultural, domestic, and industrial sewage into the aquatic environment (Müller et al., 2008; Chai et al., 2009; Yang et al., 2012; Hollert, 2013). Rapid increases in the concentrations of dissolved inorganic N (DIN) and P (DIP) have been reported, probably due to increasing fertilizer application (Zhang et al., 1999; Yu et al., 2006; Li et al., 2007; Chai et al., 2009; Yu et al., 2012). Consequently, increasing eutrophication, frequent phytoplankton blooms, and hypoxia occur in the delta and adjoining coastal waters (Han et al., 2003; Zhou et al., 2008; Chai et al., 2009; Li et al., 2016; Chen et al., 2017).

On the other hand, rapid population growth and economic development have led to the increasing need for expanding hydrological engineering infrastructure (Kuenzer et al., 2013; Tessler et al., 2015; Zarfl et al., 2015). By 2016, a total of 61,446 reservoirs had been constructed in the Yangtze River Basin (data from: http://www.stats.gov.cn/), of which the Three Gorges Dam (TGD) is the largest hydroelectric project ever built globally (Chai et al., 2009). Sediment retention caused by the operation of reservoirs and dams reduced the sediment discharge from ca. 500 Mt yr^{-1} in the 1970s to ca. 270 Mt yr^{-1} in 2002, and further decreased to ca. 100 Mt yr^{-1} in the 2010s (after TGD construction). This caused erosion and coarsening of bottom sediment in the downstream channel, and alteration of the sedimentary environment in the Yangtze River Estuary, especially regarding accretion/erosion rates, (Yang et al., 2003; Chen et al., 2005; Chen et al., 2008; Hu et al., 2009; Xu and

☆ This paper has been recommended for acceptance by Dr. Sarah Harmon.

* Corresponding author.
E-mail address: dengbing@sklec.ecnu.edu.cn (B. Deng).

https://doi.org/10.1016/j.envpol.2019.03.030
0269-7491/

Milliman, 2009; Yang et al., 2011). Nutrient fluxes have also been modified by nutrient retention within reservoirs and change in the reservation time of the river water (Gong et al., 2006; Chai et al., 2009). Furthermore, a significant reduction in the concentration of dissolved inorganic Si (DSi) has been observed during the 1960s–2000s (Yu et al., 2006; Li et al., 2007; Yu et al., 2012; Li et al., 2016; Ran et al., 2016), followed by a upturn since 2003 (Wang et al., 2018).

Nevertheless, how the environment and ecology in the estuary have responded to human activities in the Yangtze River Basin requires further evaluation. Historical monitoring data generally lack integrity and continuity, to some extent limiting the understanding of long-term variability. As the major depositional sink of biogenic components, sediment cores can provide continuous historical records of environmental changes (Treguer et al., 1995; Giblin et al., 1997; Friedl et al., 1998; Zabel et al., 1998; Yu et al., 2012). However, sediment starvation and erosion in a subaqueous delta (Yang et al., 2011) makes it relatively difficult to estimate (Colman et al., 2002). Careful analysis of sedimentary environmental change is crucial for identifying the potential sediment archive. Moreover, the decline in sediment discharge in recent decades has potentially changed the burial of C and nutrients in the river mouth and adjacent coastal area. Today, a knowledge gap remains regarding the alteration of nutrient burial fluxes and the degree to which this would affect nutrient budgets.

Therefore, in order to ascertain significant environmental changes in the Yangtze River Estuary affected by human activities and climate change over the past century, a sediment core was selected to reconstruct high resolution sediment records. The objectives of this study were to: (1) elucidate the environmental changes reflected by biogenic components, and (2) evaluate the alteration in nutrient burial fluxes and its potential impacts on nutrient cycling.

2. Materials and methods

2.1. Sample collection

Thirteen sediment cores were collected from the Yangtze River Estuary using gravity corers in July 2016 (Fig. 1). The cores were sub-sampled at 1 cm intervals using a stainless-steel knife and restored in the dark at −15 °C until further analysis. The sediments were then dried in plastic bags at 55 °C, homogenized and ground, and then subsequently analyzed for sediment dating and grain size composition. A sediment core (~243 cm in length) was finally selected that was riverine-dominated (within river the plume area) with clear deposition records, and reduced disturbance from resuspension and erosion. The core was located at the station A5-4 (31.00 °N, 122.83 °E; water depth: 30 m) in the Yangtze Delta front, which is under steady sediment accretion (Yang et al., 2011; Li et al., 2015) (Fig. 1). Core samples were further analyzed for biogenic component parameters.

2.2. Analytical methods

For grain size composition analysis, wet sediment samples were pretreated with H_2O_2 (10%) and HCl (1 M) to remove organic matter and carbonate, and then sequentially washed with Milli-Q water and disaggregated ultrasonically (Yu et al., 2012). After treatment, sediment grain size was analyzed with a Laser Particle Size Analyzer (LS13 320, Beckman Instruments Inc, USA). The measurement range of the analyzer was between 0.02 and 2000 μm, with a measurement error of <3%.

In order to calculate the sedimentation rates, a total of 18 samples were taken for the measurements of radionuclides (Bq kg^{-1}) using a HPGe γ spectroscope (GWL-120219, EG&G ORTEC, USA). The activities of total ^{210}Pb, ^{137}Cs, and ^{226}Ra were directly determined at 46.54 keV (47.43%), 661.66 keV (4.56%), and 295.21 keV (23.82%), respectively. Each sample was measured for approximately 12–24 h. Excess ^{210}Pb ($^{210}Pb_{ex}$) activity was determined by subtracting the ^{226}Ra from the total ^{210}Pb.

Total organic C (TOC), total N (TN), and their stable isotopes (^{13}C and ^{15}N) was determined using the Stable Isotope Ratio Mass Spectrometer (Delta plus XP, Thermo Finnian, USA) connected to a Flash EA 1112 analyzer. The TOC samples were acid-treated with HCl (1 M) to remove inorganic C prior to analysis, while no acid-treatment was performed for the TN samples (Zhu et al., 2014). The isotope ratios were reported in δ (‰); ^{13}C and ^{15}N were relative to the V-PDB standard and atmospheric N, respectively. The precision of the stable isotope analysis was <0.1% for C and <0.2% for N.

The analysis of biogenic Si (BSi) followed the wet-chemical digestion method (Conley, 1998). In brief, after removing organic matter and CO_3^{2-} with 5 mL of HCl (1 M) and 5 mL of H_2O_2 (10%), the dried samples (60 mg) were extracted with 30 mL of Na_2CO_3 (2 M)

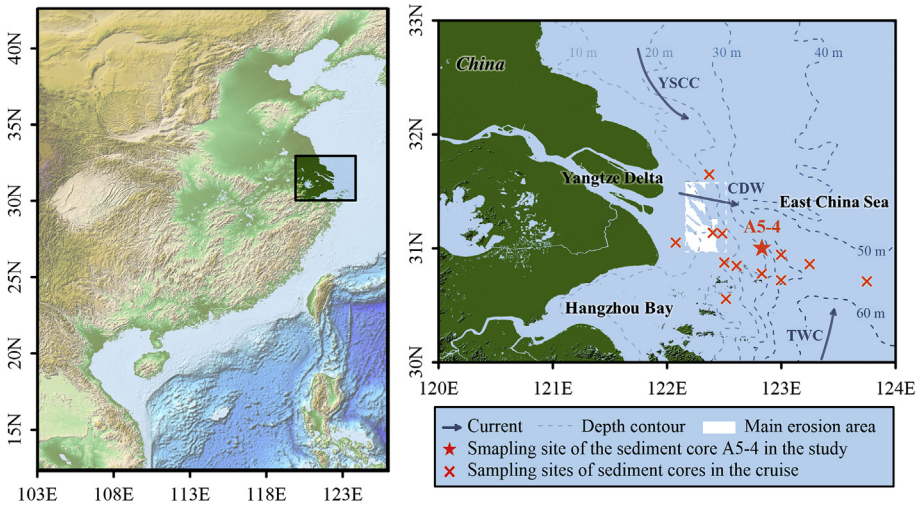

Fig. 1. Sampling sites of sediment cores and basic information the Yangtze River Estuary. The basic information of study area including accretion/erosion areas (Yang et al., 2011) and regional circulation model (arrows) (Ichikawa and Beardsley, 2002). CDW: Changjiang Diluted Water; TWC: Taiwan Warm Current; YSCC: Yellow Sea Coastal Current.

at 85 °C for 8 h. During the extraction, 0.2 mL supernatant separated from suspended material by centrifuging was removed from the extraction solution hourly. The tubes were initially treated under ultrasound before extraction in a water bath, and then shaken slightly at intervals of 10 min during the extraction. However, they were agitated vigorously after each sampling in order to resuspend the solids. All sampling steps were performed quickly in order to minimize the adsorption of DSi to solid surfaces. DSi in the extraction solution was measured by the molybdate blue spectrophotometric method (Mortlock and Froelich, 1989). The sequential extraction method with back-extrapolation of the linear section of the extraction curve was used to correct for the dissolution of co-existing aluminosilicates, following the concept that the dissolution of co-existing aluminosilicates shows a linear trend with time (DeMaster, 1981). The Chinese Coastal Sediment Reference Materials (GBW-07314) were used to assess the accuracy of biogenic Si measurements. The relative standard deviation (RSD) for six parallel samples was 3.6%, with an average recovery of 98%.

Total P (TP), inorganic P (IP), and organic P (OP) were analyzed using the ASPILA method (Aspila et al., 1976). For the TP, the sediments (50 mg) were initially ignited in the muffle furnace at 550 °C for 24 h, and then extracted with 20 mL of HCl (1 M) at 25 °C for 24 h. The procedure for measuring IP was the same except with no ignition. Dissolved P (DP) in the extractant was measured by the molybdate blue spectrophotometry method (Liu et al., 2004). The OP was obtained by subtracting the IP from the TP. The RSD for six parallel samples of the Chinese Coastal Sediment Reference Materials (GBW-07314) was 0.6%, with an average recovery of 90%.

Al was determined following classical open digestion procedures (National Environmental Bureau, 1998). The samples were then analyzed for major metal concentrations with inductively coupled plasma atomic emission spectroscopy. The RSD for parallel samples of the Chinese Stream Sediment Reference Materials (GSD-9) was 2.5%, with an average recovery within 95–105%.

3. Results

3.1. Sediment grain size composition and dating

The sediment core was dominated by silt and clay, which accounted for 40–69% and 19–40% of the total sediment, respectively. An upward-coarsening sequence was present in the sediment core, in which sediment type changed from mud and silt mud in the lower layers to sandy silt and sandy mud in the upper layers (Figs. 2 and 3). The proportion of coarser components gradually increased upwards (Fig. 3). A relatively stable average and median grain size was found at the mean levels of 6.57 μm and 12.10 μm respectively in the lower part of the sediment core (40–243 cm), with a relatively low and stable sorting coefficient. Overall increasing trends in the average and median grain sizes, and sorting coefficient occurred above 40 cm, especially in the top 20 cm (Fig. 3).

The sediment core was dated using ^{210}Pb and ^{137}Cs (Robbins and Edgington, 1975) (Fig. 4A and B). Approximate logarithmic distributions were observed in the profiles of measured and calibrated activities of excess Pb-210 ($^{210}Pb_{ex}$) in the sediment (Fig. 3E). Accordingly, the profile of the $^{210}Pb_{ex}$ logarithm was built, which suggested a piecewise linear behavior (Fig. 3G). Average deposition rates for each section were calculated using the Constant Flux Constant Sedimentation Model (CFCS) (Sanchez-Cabeza and Ruiz-Fernández, 2012) (Fig. 3G), and the chronological sequence of the sediment core was established according to average deposition rates. Based on the consideration of grain size change in the sediment core, the values of $^{210}Pb_{ex}$ and ^{137}Cs activities were calibrated by the clay fraction to eliminate the grain size effect (He and Walling, 1996). The linear behavior of three regression lines of the $^{210}Pb_{ex}$ logarithm profile in the core, coupled with the obvious linearity in each sub section, demonstrated three periods of decreasing sedimentation rates (Fig. 3G). The lowest sedimentation rate (0.22 cm yr^{-1}) occurred at the top of the sediment after 1984. It is noteworthy that the radioisotope activities in the lower core (<100 cm) were lower than the detection limit, so it could only be speculated the deposition ages according to the sedimentation rate in the adjacent section of the core (between 17 and 100 cm), which might have large uncertainty. A relatively higher sedimentation rate (0.69 cm yr^{-1}) was found between 1984 and 1970. The highest sedimentation rate (2.47 cm yr^{-1}) was observed before the 1970s. The profile of the calibrated ^{137}Cs demonstrates low activities.

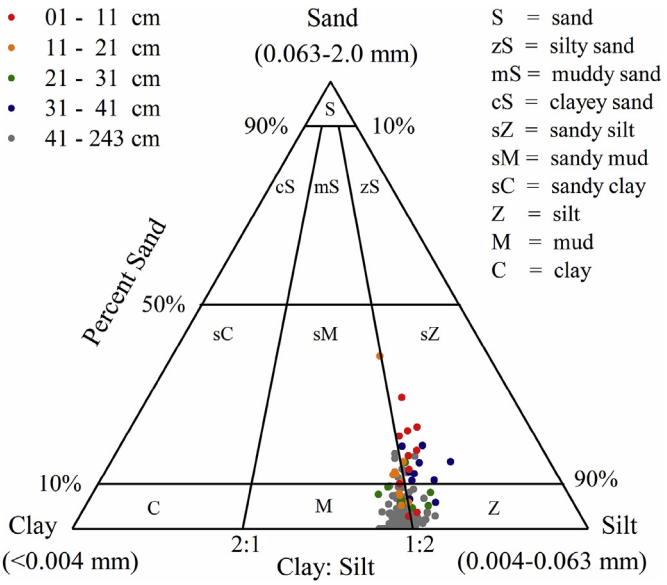

Fig. 2. Textural classification of sediments (Folk et al., 1970).

3.2. Vertical distribution of biogenic components

Based on sediment coarsening in the sediment core, the grain size effect on the biogenic components was considered. The concentration of Al in sediments is significantly correlated with grain size and/or mineral composition, and is less affected by human activities. Hence, it has been widely applied as a reference element to eliminate the granularity effect (Pilotte et al., 1978; Klinkhammer and Bender, 1981; Windom et al., 1984; Zhang et al., 1988; Liu and Zhang, 1998). In the present study, concentrations of biogenic components were calibrated by Al. Overall similarities were observed in the profiles of biogenic components: the contents of the biogenic components remained relatively stable below 65 cm (before the 1950s), while higher fluctuations occurred within the top 65 cm of the core. However, the most significant changes were mainly observed above 17 cm (after the 1970s) (Fig. 4).

The TOC contents in the core ranged from 3.53 to 6.87 mg g^{-1} (Fig. 4A). Constant change was observed in TOC before the 1950s, with a mean level of 4.64 mg g^{-1}, followed by greater fluctuation, between the 1950s and 1970s. A slight decrease in TOC initially occurred between the 1970s and 1980s. After that, a significant increase was found in the TOC profile towards the present, reaching a peak of 6.87 mg g^{-1} at the sediment surface, approximately two-fold that in the early 1980s.

The TN profile was similar to that of the TOC, with values ranging from 0.417 to 0.855 mg g^{-1} (Fig. 4B). Upwards increasing

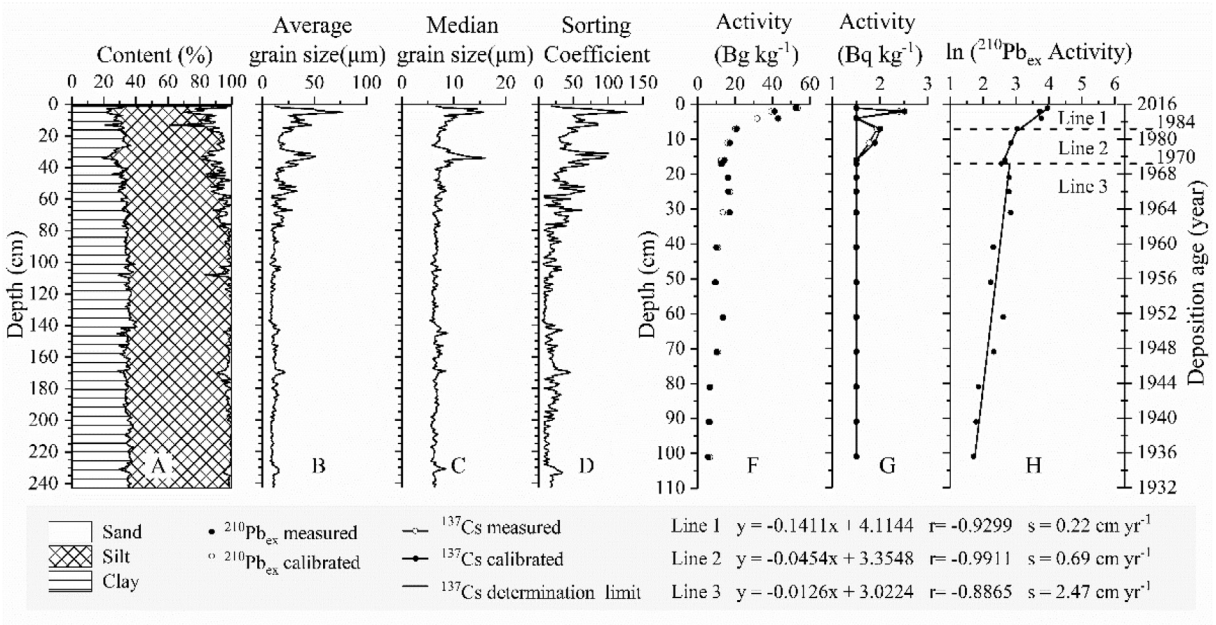

Fig. 3. The profiles of grain size parameters and sediment dating in the sediment core. (A) The composition of clay, silt and sand, (B) median diameter, (C) average diameter, (D) sorting coefficient, (E) $^{210}Pb_{ex}$ activities, (F) ^{137}Cs activities, (G) ln($^{210}Pb_{ex}$) calibrated by clay and the fitting of the CA model in the sediment core. The correlation coefficient was reported in Pearson's r. s: sedimentation rate.

fluctuations were also observed in TN. There was a decrease from 0.528 mg g^{-1} in the 1970s to 0.417 mg g^{-1} in the 1980s, followed by a two-fold increase to the present level, with TN contents peaking at 0.855 mg g^{-1} in the core surface.

A constant increase in OP was observed after the 1950s (Fig. 4F). OP content stabilized at a mean level of 0.0694 mg g^{-1} before the 1970s. It then reached its highest level of 0.106 mg g^{-1} at the surface, indicating a 1.5-fold increase at the top of the core.

IP comprised a major portion of TP, with a steady percentage ranging from 80 to 91% in the core (Fig. 4G). Hence, TP exhibited a trend similar to IP (Fig. 5D and E). The contents of TP and IP ranged from 0.457 to 0.893 mg g^{-1} and from 0.403 to 0.791 mg g^{-1}, respectively. The observed increases began with a mean level of 0.445 mg g^{-1} for IP and 0.515 mg g^{-1} for TP from the 1950s, followed by a steep increase with greater fluctuation from the 1970s, with IP and TP reaching the higher values of 0.583 and 0.719 mg g^{-1} at the surface, respectively. Peaks occurred in the early 1990s with values of 0.893 and 0.791 mg g^{-1} for TP and IP, respectively.

BSi contents in the core also indicated a trend similar to TOC and TN, ranging from 7.48 to 12.0 mg g^{-1} (Fig. 4C). However, the increase in BSi at the top of core was not as large as those of TOC and TN. Relatively steady BSi contents were presented in the lower profile before the 1950s at a mean level of 9.19 mg g^{-1}. There was a slow increase between the 1950s and 1970s, followed by a decrease and then an increase until present, with BSi content reaching a relative peak of 10.3 mg g^{-1} (lower than that in the 1970s) at the surface.

A constant increase was found in the $\delta^{13}C$ profile from the 1950s (Fig. 4H). A stable state of $\delta^{13}C$ was observed in the lower core before the 1950s, with values fluctuating between −24.88‰ and −23.55‰. This was followed by an increase in $\delta^{13}C$, reaching the highest value of −22.80‰ at the surface. Conversely, a reduction was found in $\delta^{15}N$ from the 1920s, with values changing from 6.111‰ in 1920 to 4.132‰ in 1967 (Fig. 4I). After this, $\delta^{15}N$ stabilized at a relative low level of 4.724‰ at the top of the core, with an exception of a peak in the mid-1980s.

4. Discussion

4.1. Chronology and sedimentary environment change

The average sedimentation rates and corresponding chronologies obtained by sediment dating can be used to reconstruct records of the sedimentary environment. In the present study, the highest average sedimentation rate of 2.47 cm yr^{-1} was found in the lower part of the core before the 1970s (Fig. 5A). During this period, the recorded Yangtze River sediment discharge reached approximately 500 million tons per year according to hydrological observations (Changjiang Water Resources Commission of the Ministry of Water Resources, 2017). Large amounts of sediment discharge to the river mouth induced rapid accretion of the shoreline (DeMaster et al., 1985), with a maximum submerged delta aggradation, which was reported to be as high as 5 cm per year (Milliman et al., 1985).

Subsequent decreasing sedimentation rates of 0.69 cm yr^{-1} and 0.22 cm yr^{-1} in the delta front from the 1970s–1980s and from 1980s to present, respectively, were consistent with long-term monitoring riverine sediment discharge data (Fig. 5A). According to the data from Datong Hydrology Station, which is a controlling station for measurements of water and sediment discharge from the Yangtze River into the sea, sediment discharge showed a decreasing trend from the 1970s (Fig. 5A). The decrease in the sediment discharge occurred in the late 1970s with the construction of the large hydrological infrastructures (Pang et al., 2011) (Fig. 6A). Consequential lower sediment discharge between the early-1970s and mid-1980s was approximately 440 Mt yr^{-1}, accounting for 90% of the mean load in the latter period. A sharp decrease then occurred from the mid-1980s with the operation of more hydrological infrastructures including the Gezhou Dam and the TGD (Yang and Chen, 2007) (Fig. 6A). Corresponding erosion occurred in the partial subaqueous delta generated by sediment starvation. The erosion was observed primarily between 5 m and 8 m below the lowest tide from 2000 (Yang et al., 2011). Although the core in the present study was located in the Yangtze Delta front

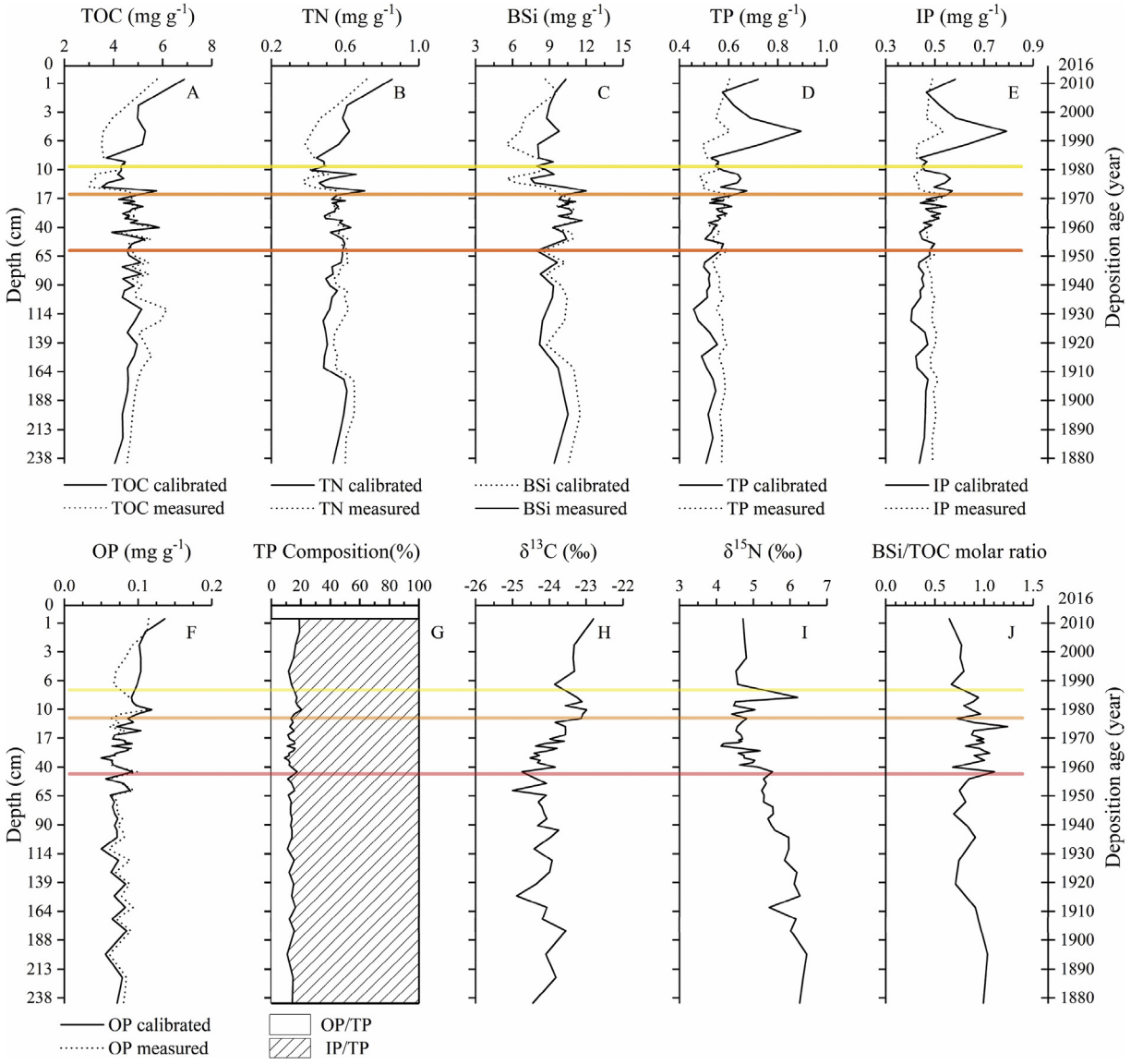

Fig. 4. The profiles of biogenic components in the sediment core. (A) TOC, (B) TN, (C) BSi, (D) TP, (E) IP, (F) OP, (G) Proportions of IP and OP in TP, (H) ^{13}C, (I) ^{15}N, (J) TOC/BSi molar ratio. $C_{calibrated(i)} = C_{measured(i)}/C_{Al(i)}/C_{Al(average)}$; $C_{calibrated(i)}$: the contents of biogenic components calibrated by Al in layer (i) (cm); $C_{measured/Al(i)}$: the measured contents of biogenic components/Al in layer (i) (cm); $C_{Al(average)}$: the average content of Al in the sediment core.

at a water depth of 30 m, no obvious erosion was observed. However, the change in sedimentation rate suggested that the decline in submerged delta accretion probably began in the 1980s immediately following the decrease in sediment supply from the river basin. Similar decrease in sedimentation rates from 5.1 cm yr^{-1} in 1958–1978 to 0.2 cm yr^{-1} in 1978–1997 in the outer subaqueous delta (separated by 122.3 °E) was reported (Yang et al., 2003). The decreased sedimentation rates responded to the reduction in sediment discharge caused by the hydrological infrastructures, indicating that the human activities have changed the sedimentary environments in the Yangtze River Estuary, where the sedimentary environment was demonstrated to be dominated by sediment delivery from the river basin. It also implied that high resolution sediment records could be reconstructed in the delta front as the core A5-4.

The grain size coarsening in the sediment core might also be the result of the decrease in sediment discharge. The stable grain size composition with less fluctuation in the lower core corresponded to the early period with high speed accretion in the delta front (Fig. 3). Subsequent increasing fluctuation in grain size and coarsening corresponded to the decreasing Yangtze sediment discharge and its consequential increasing resuspension-dominated environment (Milliman et al., 1985; Zhuang, 2005; Luo, 2012; Yang et al., 2018). Coarsening of the Yangtze channel sediment has been reported to suggest erosion along the middle reaches of the river since 2003 (Yang et al., 2011). Corresponding coarsening of suspended sediments from the Yangtze River to the East China Sea was also observed, in addition to the erosion of the subaqueous delta off the Yangtze River mouth, causing the coarsening of seabed sediments after the construction of the TGD (Luo et al., 2012). However, the present results in the delta front suggested that the coarsening and decline in delta accretion probably began in the 1980s, which was much earlier than TDG construction. The difference was presumably because the delta front was more sensitive to change in sediment supply to the river mouth compared with the main submerged delta (Yang et al., 2018).

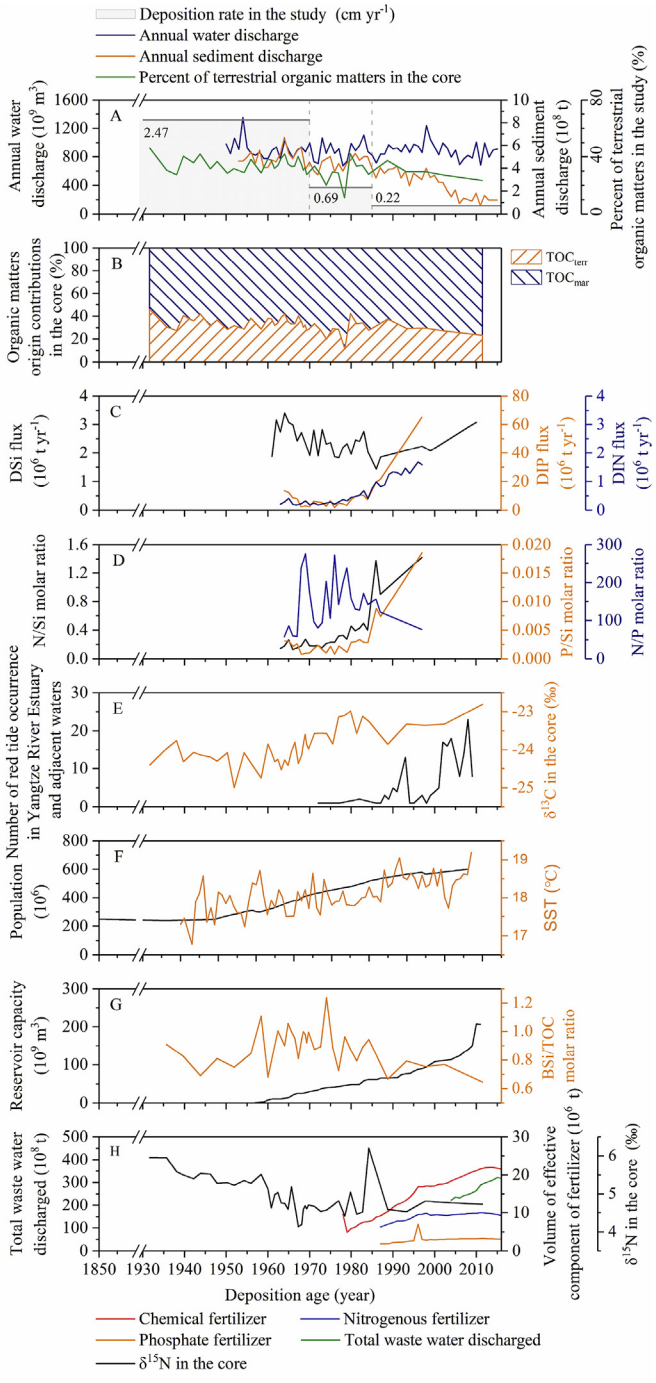

Fig. 5. Records of natural and anthropogenic background in the Yangtze River Basin and Estuary. (A) The annual water and sediment discharges monitored by Datong Hydrology Station (data from: Changjiang Water Resources Commission of the Ministry of Water Resources (2017)), compared with the sedimentation rates and percent of terrestrial organic matters in the study. (B) The organic matter provenance composition proportion estimated by the least squares method model in the study. TOC_{terr}: terrestrial organic matter; TOC_{mar}: marine organic matter. (C) Inter-annual variations of fluxes of DSi, DIP and DIN monitored by Datong Hydrology Station (data from: Li et al. (2007) and Wang et al. (2018)). (D) Inter-annual variations of N/Si, P/Si and N/P molar ratios monitored by Datong Hydrology Station (data from: Li et al. (2007)). (E) Number of red tide occurrences in Yangtze River Estuary and adjacent waters (data from: Liu et al. (2013)), compared with the $\delta^{13}C$ in the study. (F) Population in the Yangtze River Basin (modified after Zhang (2006), http://www.stats.gov.cn/) and the annual sea surface temperature(SST) in the study area. Annual Extended Reconstructed SST Version 3b (ERSST V3b) (Smith et al., 2008; Xue et al., 2003), ERSST V4 (Huang et al., 2015; Liu et al., 2015) and ERSST V5 (Huang et al., 2017) are provided by the NOAA/OAR/ESRL PSD, Boulder, Colorado, USA, from their Web site at https://www.esrl.noaa.gov/psd/. Ensemble mean of different datasets is employed to reduce errors in the observations and to best represent the truth of the real world. And all these three datasets have a horizontal resolution of 2.0° × 2.0°. (G) Reservoir capacity in the Yangtze River Basin (data from: Xu et al. (2013)), compared with the BSi/TOC molar ratio in the study. (H) Total waste water discharge and volume of effective component of fertilizer in the Yangtze River Basin (data from: http://www.stats.gov.cn/), compared with the $\delta^{15}N$ in the study.

4.2. Changes in nutrients and primary productivity in the Yangtze River Estuary

The fluctuation of biogenic components along with variations in grain size composition and sedimentation rate in the sediment profile suggested significant environmental changes during the past several decades (Figs. 3–5).

Due to abundant sediment supply from the large turbid river, the estimated sedimentation rates in the present study were relatively higher than those of an average coastal region. To some extent, this high sedimentation rate favorited the preservation of organic matter in sediments. In addition, the profiles of TOC and TN which are usually affected by early diagenesis showed similar variations to those of OP and BSi (Fig. 5A–C, and F), indicating that the core was minorly affected by early diagenesis. Thus, the vertical distributions of the biogenic components were mainly influenced by environmental changes including riverine input of nutrients and *in situ* primary productivity.

Before the 1950s, a relatively stable state and low fluctuation of biogenic components (Fig. 4) suggested a minor influence of human activities. A relatively lower and stable population (Fig. 5F) implied that the variation in nutrients resulted from climatic- or natural process-dominated changes. However, $\delta^{15}N$ (Fig. 4I) was the exception as it showed a slow decrease from the early 20th century. Due to the complexity of influencing factors and the lack of relevant data records, it was difficult to distinguish and conclude the controlling factors of $\delta^{15}N$ reduction in this period.

Slight increases in OP, BSi, TN, and TOC (Fig. 5A–C, and F) began during the 1950s–1970s, suggesting increased nutrient deposition in the delta front. Meanwhile, $\delta^{13}C$ (Fig. 4H) inclined towards a marine organic origin. Furthermore, $\delta^{15}N$ (Fig. 4I) became lighter, corresponding to the increase in fertilizer application (Fig. 5H) in the river basin. According to the statistics, NO_3^{1-} nitrogenous fertilizer application in the Yangtze River Basin began in the 1950s (Yan et al., 2001). Thereafter, the quantity of N fertilizer application was reported to increase rapidly, from several 100,000 tons per year in the 1960s to 2–3 million tons per year in the 1970s (Yan et al., 2001). Moreover, according to the statistics, the population (Fig. 5F) in the Yangtze River Basin underwent a rapid increase from 248 million in 1949 to 381 million in 1970. Accordingly, this resulted in increasing nutrient input into river and estuarine water. Riverine DIP and DIN fluxes (Fig. 5C) multiplied during this period (Li et al., 2007). As a result, the increase in $\delta^{13}C$ (Fig. 4H) could indicate the consequential increase in primary productivity. Chemical fertilizer application accompanying the population growth substantially increased nutrient fluxes to the river mouth, thereby stimulating a higher level of primary productivity. Since then, the impact of human activities on riverine and estuarine ecosystems has gradually surpassed that of climate change.

Slight reductions in TOC, TN, and BSi (Fig. 5A–5C) occurred during the late 1970s–1980s. However, OP, $\delta^{13}C$, and $\delta^{15}N$ (Fig. 5F, H, and I) remained at high tropic levels. The diversification of biogenic components was presumably related to the operation of large hydrological infrastructures in the Yangtze River Basin. Dam operation in the river basin trapped not only sediment that resulted in a reduction in sediment charge (thereby coarsening the sediment in the present study's core) and deposition, but also terrestrial

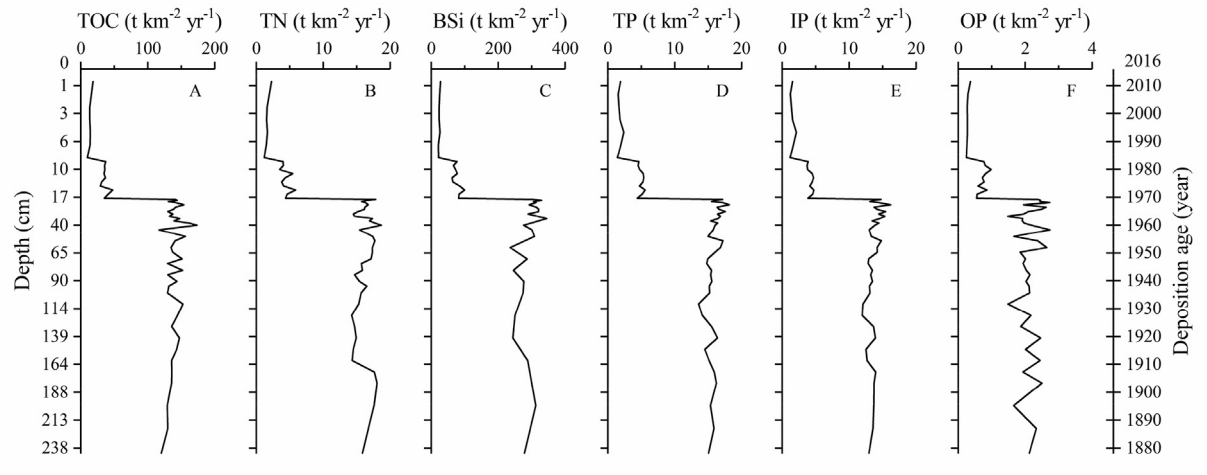

Fig. 6. The profiles of burial fluxes of biogenic components in the sediment core. (A) TOC, (B) TN, (C) BSi, (D) TP, (E) IP, (F) OP. Burial fluxes (t km^{-2} yr^{-1}) = the contents of biogenic components*average sedimentation rate* dry bulk density. The value of dry bulk density was chose to be 1.2 g cm^{-3} (Keller and Ye, 1985; Chung and Chang, 1995; Lin et al., 2002; Deng et al., 2006).

organic matter that may be responsible for the reduction in TOC and TN (Fig. 5A and B). A similar correlation regarding the decline in terrestrial organic matter with riverine sediment discharge was also revealed by long-term monitoring data (Yu et al., 2011). Moreover, the decline in BSi (Fig. 4C) in this period probably resulted from the damming retention effect due to the increased reservation time of river water and consequent consumption and sedimentation of the DSi in the reservoirs (Duan et al., 2007; Wang et al., 2018). The same processes were also found in the Danube River after operation of the Iron Gates Dam (Humborg et al., 1997).

Since the late 1980s, significant increases in TOC, TN, OP, and BSi (Fig. 5A–C, and F) revealed that the growth of primary productivity stimulated by eutrophication might be the prevailing controlling factor of the distribution of biogenic components, over the impact of sedimentary adjustment caused by hydrological infrastructures. In this period, there was over a three-fold increase in fertilizer application from 1980 to 2016 (Fig. 5H). However, the relatively stable state of $\delta^{15}N$ at the top of the core, rather than a reduction, might be the result of both NO_3^{1-} fertilizer application and the discharge of agricultural, domestic, and industrial sewage. The statistics showed that the total waste water discharge in the Yangtze River Basin increased from 22 billion tons in 2004 to 317 billion tons in 2016 (Fig. 5H). Correspondingly, abrupt increases in N and P riverine loads were found in the monitoring data at Datong station. It was reported that the DIP flux of the Yangtze River increased from approximately 7 million tons per year in the early 1980s to approximately 65 million tons per year in the late 1990s, while the DIN flux increased from approximately 0.4 million tons per year in the early 1970s to approximately 1.6 million tons per year in the late 1990s (Li et al., 2007) (Fig. 5C). Increasing nutrient levels in the water aggravated eutrophication and consequently stimulated marine primary productivity. A 10–20 fold increase in cell abundance of dominant phytoplankton was observed in the Yangtze River Estuary and its coastal waters from the beginning of the 1980s to the mid-1990s and the early of 21st century (Wang et al., 2004). Chai et al. (2006) reported increasing mean concentration of Chl *a* in the Yangtze River Estuary by comparing data from 1986 to 2004, and the spring/summer Chl *a* maximum in 2002 was nearly four-fold as high as that in 1986. In addition, decreased suspended particulate matter concentrations in the Yangtze River and its estuary, caused by the reduction in sediment discharge, might have also promoted phytoplankton growth via the enhancement of water body transparency (Sullivan et al., 2001; Coynel et al., 2005; Duan and Bianchi, 2006; Yu et al., 2011).

However, the influence of the development of hydrological infrastructures during this stage was also reflected in the nutrient molar ratio. BSi is considered to be a good proxy of diatom production, which is an important component of primary production (Ragueneau et al., 1996; Conley and Schelske, 2002). The increases in TOC and TN (Fig. 5A and B) substantially outpaced BSi (Fig. 4C) at the upper core. The BSi/TOC molar ratio was calculated for qualitative assessments of diatom primary productivity. The decrease in the BSi/TOC molar ratio first presented in the 1980s, and continued to decrease (Fig. 4J). The continued change in the BSi/TOC molar ratio in the Yangtze Delta sediments suggested a reduction in diatom productivity in the previous decades. It has been reported that the adjustment of Danube nutrient fluxes after reservoir impoundment were immediate (Humborg et al., 1997). The long-term changing tendency of the BSi/TOC molar ratio negatively correlated with total reservoir capacity increase over the past 40 years (Fig. 5G). According to the monitoring data at Datong station, the significant decline in DSi of the Yangtze River started in the 1980s (Li et al., 2007) (Fig. 5C). Although, there was an upturn of DSi flux since 2003 (Wang et al., 2018), which is consistent with the increase in BSi at the top of the core in this study, the continued drop in BSi/TOC molar ratio might still indicate the decreasing diatom productivity percentage. The retention of silicate in the reservoirs, combined with the eutrophication tendency, altered the structure of nutrient loads in the water (Fig. 5D), and further led to shifts in phytoplankton species composition from diatoms to non-diatoms in the Yangtze River Estuary. Correspondingly, the dominant species in red tides has been reported to transition from diatoms to non-diatoms. For example, the percentage of *Skeletonema costatum* in red tides decreased from 33.3% in 1980–1989 to 24% in 2000–2002 (Li et al., 2007).

Table 1
The estimated average burial fluxes (t km^{-2} yr^{-1}) of biogenic components in different period in the study.

Period	TOC	TN	BSi	TP	IP	OP
After the mid-1980s	13.7	1.62	23.8	3.97	3.37	0.604
During the 1970s to mid-1980s	36.3	4.39	76.8	10.7	9.12	1.60
Before the 1970s	140	16.2	181	34.3	29.6	4.62

Table 2
Burial fluxes (t km^{-2} yr^{-1}) of biogenic components in Deltas and Marginal Seas.

Region	TOC	TN	BSi	TP	IP	OP
The Bohai Sea	2.4–21.6[a]	–	5.6–22.4[a]	0.353–23.4[b]	0.24–19.2[b]	0.059–4.22[b]
	1.35–132[c]	0.13–14.58[c]	4.82–245[c]	0.27–34.69[c]	0.23–28.40[c]	0.04–6.28[c]
The Yellow Sea	12.6[e]	–	5.6–33.6[d]	0.17–1.92[b]	0.16–1.43[b]	0.01–0.59[b]
The Southern Yellow Sea	–	0.39–2.36[f]	–	–	–	–
The North Sea	1.75[g]	–	–	0.014[h]	–	–
The Southern North Sea	–	19.1[i]	–	11.2–25.2[j]	–	–
The Mississippi Delta	64[k]	6.0–23[l]	20.47[m]	–	–	0.7–2.1[n]
The Arabian Sea	–	–	–	0.01–0.22[o]	–	–
The Eastern Arabian Sea	0.8–21[p]	0.08–2.47[p]	–	–	–	–
The Northern Arabian Sea	–	–	0.31–1.32[q]	–	–	–
The Baltic Sea	1.197[r]	2.08[s]	12–24[t]	–	–	–
The North-western Baltic Proper coastal zone	–	–	–	1.7–2.8[u]	–	–

Data from.
[a] Liu et al. (2018).
[b] Liu et al. (2004).
[c] Jiang (2012).
[d] Liu et al. (2016).
[e] Hu et al. (2016).
[f] Lü et al. (2005).
[g] de Haas and van Weering (1997).
[h] Brion et al. (2004).
[i] Oehler et al. (2015a).
[j] Oehler et al. (2015b).
[k] Turner et al. (2004).
[l] Smith et al. (1985).
[m] Presti and Michalopoulos (2008).
[n] Ingall and Van Cappellen (1990).
[o] Schenau and De Lange (2001).
[p] Bhushan et al. (2001).
[q] van der Weijden and van der Weijden (2002).
[r] Winogradow and Pempkowiak (2014).
[s] Thomas et al. (2010).
[t] Olli et al. (2008).
[u] Rydin et al. (2011).

In addition, the impact of global climate change should not be neglected. In the context of climate change, increasing atmospheric and ocean temperature might alter precipitation, weathering, runoff, ocean stratification, ocean acidity, patterns of ocean circulation, and nutrient levels, further affecting the environments and ecosystems of the river basin and estuary (Hoegh-Guldberg and Bruno, 2010; Lü et al., 2017). With the development of global warming, the sea surface temperature (SST) in the Yangtze River Estuary has shown a significant increase, which might be one of the factors of the environment change (Fig. 6F). Although the complexity of ecological interactions makes it difficult to determine the total impacts adequately, global climate change can enhance the detrimental effects of human activities according to several case studies (Walther et al., 2002).

4.3. Changes of nutrient and organic carbon burial

Biogenic component burial fluxes in the core were estimated by combining the contents with sedimentation rates (Fig. 6 and Table 1), showing considerable change over the last several decades. The high resolution sediment records revealed not only environmental changes during the previous decades, but also the potential nutrient burial variation in the context of river sediment starvation. Maximum burial fluxes were recorded in the lower core (before the 1970s) (Fig. 6 and Table 1), with values of 140, 16.2, 181, and 4.62 t km^{-2} yr^{-1} for TOC, TN, BSi, and OP, respectively. These burial fluxes were significantly higher than the average shelf and coastal environment values (Tables 1 and 2). High nutrient burial fluxes were presumably due to rapid sediment deposition that favored nutrient preservation. Hence, substantial nutrient burial ensured efficient nutrient removal from the water column, which is essential for delta ecosystems and services (Giosan et al., 2014). The estimated burial fluxes declined dramatically during the 1970s–1980s by 60–70% compared with those before the 1970s (Fig. 6 and Table 1), though the concentrations increased during this period. Minimum burial fluxes were presented in the upper core (after the late 1980s), whilst the burial fluxes were one order of magnitude lower than those before the 1970s, despite the rapid increase in concentration during this period. The significant positive correlation of nutrient burial fluxes with sedimentation rates indicated that it was the later that dominated the burial fluxes. While little attention has been paid to nutrient burial fluxes, previous estimation of the long-term OC burial rate for the East China Sea Shelf (14.7 t km^{-2} yr^{-1}, Deng et al., 2006) was similar to the present result (13.6 t km^{-2} yr^{-1}) (Table 1).

Despite the fact that the present study was only based on a single core from the delta front, our findings may represent an average and/or an optimistic estimation on recent nutrient burial and removal in the Yangtze Delta region. According to long-term morphological calculation (Yang et al., 2011) and *in situ* sedimentary dynamic observation (Deng et al., 2017), net sediment erosion occurred from 2003 due to the decrease in sediment discharge. The erosion appears mostly within a depth of 20 m (Yang et al., 2011), while the delta front is still under sediment balance or accretion where nutrient burial remains.

Recent decline in nutrients and C storage in the Yangtze Delta area imply a low trap efficiency of this region for nutrient removal. More than 90% of buried nutrients may have been further transported along the diluted water disperse path by tides and currents to the inner shelf and open waters. Correspondingly, increasing nutrient influxes from the Yangtze River Basin further increased the degree and scope of eutrophication in the coastal area. Recent

research has reported a higher frequency and larger extension of algae blooms (red tide) in the adjoining coastal and shelf region (Zhou et al., 2008; Wang and Wu, 2009; Liu et al., 2013; Jiang et al., 2014) (Fig. 5E). Though their nutrient source and biological dynamics still require further investigation, changes in the trap efficiency of delta sediments are likely to be one of the most important factors.

Because sediment starvation in river deltas is common worldwide due to the increase in hydrological engineering for the pursuit of clean energy and fresh water resources (Milliman, 1997; Syvitski et al., 2005), its influences on nutrient burial, and consequently nutrient cycles, of coastal regions warrants further attention and evaluation.

5. Conclusions

Nutrient changes in the Yangtze Delta front sediment profile were coincident with increased human activities in the watershed during previous decades. This suggested that the delta shifted from a natural climate change prevailing system towards an anthropogenic-dominated one.

Increases in OP, BSi, TN, and TOC began in the 1950s, along with $\delta^{13}C$ depletion towards a marine organic origin, and reduction in $\delta^{15}N$. This indicated that strengthened anthropogenic activities including chemical fertilizer application and population growth increased nutrients fluxes to the river mouth and stimulated primary productivity over that of natural weathering dominated fluctuations.

The depletion of TOC, TN, and BSi since the 1980s, together with the decline in sedimentation rate and coarsening of sediment in the profile, was largely consistent with increasing hydrological engineering practices in the river basin. Sediment retention caused by the operation of reservoirs and dams reduced the sediment discharge of the Yangtze River. This resulted in sediment coarsening and reduction in sedimentation rate, and riverine TOC and TN influxes in the Yangtze River Estuary. The variations in the BSi/TOC molar ratio were most likely attributed to the change in primary productivity toward non-diatom species. The trap of Si in the reservoirs substantially decreased the riverine discharge downstream to the river mouth, and consequently modified primary productivity in the delta.

Nutrient and organic C burial fluxes were mainly constrained by sedimentation rate, rather than nutrient influxes and primary productivity. Recent dramatic decline in nutrients and C burial in the delta area suggested low efficiency for nutrient removal in this area. Consequently, more nutrients have been further transported to the inner shelf and open waters instead of being buried in the delta sediment.

Acknowledgement

The research was funded by the China National key research and development program (grant No. 2016YFA0600904), and the Natural Science Foundation of China (grant No. 41271519, 41725002). The authors appreciate assistant by crew members of research vessel RungJiang for sediment core drilling during 2016 summer public cruise funded by the Natural Science Foundation of China. The authors thank Prof. D.Y. Liu for assistance in SST data analysis.

References

Aspila, K.I., Agemian, H., Chau, A.S.Y., 1976. A semi-automated method for the determination of inorganic, organic and total phosphate in sediments. Analyst 101, 187–197. https://doi.org/10.1039/AN9760100187.

Bhushan, R., Dutta, K., Somayajulu, B.L.K., 2001. Concentrations and burial fluxes of organic and inorganic carbon on the eastern margins of the Arabian Sea. Mar. Geol. 178, 95–113. https://doi.org/10.1016/S0025-3227(01)00179-7.

Bianchi, T.S., Allison, M.A., 2009. Large-river delta-front estuaries as natural "recorders" of global environmental change. P. Natl. A. Sci. 106, 8085–8092. https://doi.org/10.1073/pnas.0812878106.

Brion, N., Baeyens, W., De Galan, S., Elskens, M., Laane, R.W.P.M., 2004. The North Sea: source or sink for nitrogen and phosphorus to the Atlantic Ocean? Biogeochemistry 68, 277–296. https://doi.org/10.1023/B:BIOG.0000031041.38663.aa.

Chai, C., Yu, Z.M., Shen, Z.L., Song, X.X., Cao, X.H., Yao, Y., 2009. Nutrient characteristics in the Yangtze River estuary and the adjacent East China sea before and after impoundment of the three Gorges dam. Sci. Total Environ. 407, 4687–4695. https://doi.org/10.1016/j.scitotenv.2009.05.011.

Chai, C., Yu, Z.M., Song, X.X., Cao, X.H., 2006. The status and characteristics of eutrophication in the Yangtze River (Changjiang) estuary and the adjacent East China sea, China. Hydrobiologia 563, 313–328. https://doi.org/10.1007/s10750-006-0021-7.

Changjiang Water Resources Commission of the Ministry of Water Resources, 2017. Changjiang Sediment Bulletin. Changjiang Press, Wuhan, 2016.

Chen, C., Mao, Z.Z., Tang, F.P., Han, G.Q., Jiang, Y.Z., 2017. Declining riverine sediment input impact on spring phytoplankton bloom off the Yangtze River Estuary from 17-year satellite observation. Cont. Shelf Res. 135, 86–91. https://doi.org/10.1016/j.csr.2017.01.012.

Chen, X.Q., Yan, Y.X., Fu, R.S., Dou, X.P., Zhang, E.F., 2008. Sediment transport from the Yangtze River, China, into the sea over the post-three gorge dam period: a discussion. Quatern. Int. 186, 55–64. https://doi.org/10.1016/j.quaint.2007.10.003.

Chen, X.Q., Zhang, E.F., Mu, H.Q., Y, Z., 2005. A preliminary analysis of human impacts on sediment discharges from the Yangtze, China, into the sea. J. Coastal Res. 21, 515–521. https://doi.org/10.2112/03-0034.1.

Chung, Y., Chang, W.C., 1995. Pb-210 fluxes and sedimentation rates on the lower continental slope between Taiwan and the South Okinawa Trough. Cont. Shelf Res. 15, 149–164. https://doi.org/10.1016/0278-4343(94)E0023-F.

Colman, S.M., Baucom, P.C., Bratton, J.F., Cronin, T.M., McGeehin, J.P., Willard, D., Zimmerman, A.R., Vogt, P.R., 2002. Radiocarbon dating, chronologic framework, and changes in accumulation rates of Holocene estuarine sediments from Chesapeake Bay. Quaternary Res. 57, 58–70. https://doi.org/10.1006/qres.2001.2285.

Conley, D.J., 1998. An interlaboratory comparison for the measurement of biogenic silica in sediments. Mar. Chem. 63, 39–48. https://doi.org/10.1016/S0304-4203(98)00049-8.

Conley, D.J., Schelske, C.L., 2002. Biogenic silica. In: Smol, J.P., Birks, H.J.B., Last, W.M., Bradley, R.S., Alverson, K. (Eds.), Tracking Environmental Change Using Lake Sediments. Springer, Dordrecht, pp. 281–293.

Coynel, A., Seyler, P., Etcheber, H., Meybeck, M., Orange, D., 2005. Spatial and seasonal dynamics of total suspended sediment and organic carbon species in the Congo River. Global Biogeochem. CY 19. https://doi.org/10.1029/2004GB002335.

de Haas, H., van Weering, T.C.E., 1997. Recent sediment accumulation, organic carbon burial and transport in the northeastern North Sea. Mar. Geol. 136, 173–187. https://doi.org/10.1016/S0025-3227(96)00072-2.

DeMaster, D.J., 1981. The supply and accumulation of silica in the marine environment. Geochim. Cosmochim. AC 45, 1715–1732. https://doi.org/10.1016/0016-7037(81)90006-5.

DeMaster, D.J., McKee, B.A., Nittrouer, C.A., Qian, J.C., Cheng, G.D., 1985. Rates of sediment accumulation and particle reworking based on radiochemical measurements from continental shelf deposits in the East China Sea. Cont. Shelf Res. 4, 143–158. https://doi.org/10.1016/0278-4343(85)90026-3.

Deng, B., Wu, H., Yang, S.L., Zhang, J., 2017. Longshore suspended sediment transport and its implications for submarine erosion off the Yangtze River Estuary. Estuar. Coast Shelf Sci. 190, 1–10. https://doi.org/10.1016/j.ecss.2017.03.015.

Deng, B., Zhang, J., Wu, Y., 2006. Recent sediment accumulation and carbon burial in the East China Sea. Global Biogeochem. CY 20. https://doi.org/10.1029/2005GB002559.

Duan, S.W., Bianchi, T.S., 2006. Seasonal changes in the abundance and composition of plant pigments in particulate organic carbon in the lower Mississippi and Pearl Rivers. Estuar. Coast 29, 427–442. https://doi.org/10.1007/BF02784991.

Duan, S., Xu, F., Wang, L.-J., 2007. Long-term changes in nutrient concentrations of the Changjiang River and principal tributaries. Biogeochemistry 85, 215–234. https://doi.org/10.1007/s10533-007-9130-2.

Folk, R.L., Andrews, P.B., Lewis, D.W., 1970. Detrital sedimentary rock classification and nomenclature for use in New Zealand. New Zeal. J. Geol. Geop. 13, 937–968. https://doi.org/10.1080/00288306.1970.10418211.

Friedl, G., Dinkel, C., Wehrli, B., 1998. Benthic fluxes of nutrients in the northwestern Black Sea. Mar. Chem. 62, 77–88. https://doi.org/10.1016/S0304-4203(98)00029-2.

Giblin, A.E., Hopkinson, C.S., Tucker, J., 1997. Benthic metabolism and nutrient cycling in Boston Harbor, Massachusetts. Estuaries 20, 346–364. https://doi.org/10.2307/1352349.

Giosan, L., Syvitski, J., Constantinescu, S., Day, J., 2014. Climate change: protect the world's deltas. Nature 516, 31–33. https://doi.org/10.1038/516031a.

Gong, G.-C., Chang, J., Chiang, K.-P., Hsiung, T.-M., Hung, C.-C., Duan, S.-W., Codispoti, L.A., 2006. Reduction of primary production and changing of nutrient ratio in the East China sea: effect of the three Gorges dam? Geophys. Res. Lett. 33. https://doi.org/10.1029/2006GL025800.

Han, X.R., Wang, X.L., Sun, X., Shi, X.Y., Zhu, C.J., Zhang, C.S., Lu, R., 2003. Nutrient distribution and its relationship with occurrence of red tide in coastal area of

East China Sea. Chinese J Appl Ecol 14, 1097–1101. https://doi.org/10.13287/j.1001-9332.2003.0245.
He, Q., Walling, D.E., 1996. Interpreting particle size effects in the adsorption of ^{137}Cs and unsupported ^{210}Pb by mineral soils and sediments. J. Environ. Radioactiv. 30, 117–137. https://doi.org/10.1016/0265-931X(96)89275-7.
Hoegh-Guldberg, O., Bruno, J.F., 2010. The impact of climate change on the world's marine ecosystems. Science 328, 1523–1528. https://doi.org/10.1126/science.1189930.
Hollert, H., 2013. Processes and environmental quality in the Yangtze river system. Environ. Sci. Pollut. R 20, 6904–6906. https://doi.org/10.1007/s11356-013-1943-z.
Hu, B.Q., Yang, Z.S., Wang, H.J., Sun, X.X., Bi, N.S., Li, G.G., 2009. Sedimentation in the three Gorges dam and the future trend of Changjiang (Yangtze River) sediment flux to the sea. Hydrol. Earth Syst. SC 13, 2253–2264. https://doi.org/10.5194/hess-13-2253-2009.
Hu, L.M., Shi, X.F., Bai, Y.Z., Qiao, S.Q., Li, L., Yu, Y.G., Yang, G., Ma, D.Y., Guo, Z.G., 2016. Recent organic carbon sequestration in the shelf sediments of the Bohai Sea and Yellow Sea, China. J. Marine Syst. 155, 50–58. https://doi.org/10.1016/j.jmarsys.2015.10.018.
Huang, B., Banzon, V.F., Freeman, E., Lawrimore, J., Liu, W., Peterson, T.C., Smith, T.M., Thorne, P.W., Woodruff, S.D., Zhang, H.-M., 2015. Extended reconstructed sea surface temperature version 4 (ERSST. v4). Part I: upgrades and intercomparisons. J. Climate 28, 911–930. https://doi.org/10.1175/Jcli-D-14-00006.1.
Huang, B., Thorne, P.W., Banzon, V.F., Boyer, T., Chepurin, G., Lawrimore, J.H., Menne, M.J., Smith, T.M., Vose, R.S., Zhang, H.-M., 2017. Extended reconstructed sea surface temperature, version 5 (ERSSTv5): upgrades, validations, and intercomparisons. J. Climate 30, 8179–8205. https://doi.org/10.1175/Jcli-D-16-0836.1.
Humborg, C., Ittekkot, V., Cociasu, A., Bodungen, B.v., 1997. Effect of Danube River dam on black sea biogeochemistry and ecosystem structure. Nature 386, 385–388. https://doi.org/10.1038/386385a0.
Ichikawa, H., Beardsley, R.C., 2002. The current system in the Yellow and East China seas. J. Oceanogr. 58, 77–92. https://doi.org/10.1023/A:1015876701363.
Ingall, E.D., Van Cappellen, P., 1990. Relation between sedimentation rate and burial of organic phosphorus and organic carbon in marine sediments. Geochim. Cosmochim. AC 54, 373–386. https://doi.org/10.1016/0016-7037(90)90326-G.
Jiang, H.H., 2012. Study on Biogenic Elements in Sediments of the Bohai Sea. The Ocean University of China.
Jiang, Z.B., Liu, J.J., Chen, J.F., Chen, Q.Z., Yan, X.J., Xuan, J.L., Zeng, J.N., 2014. Responses of summer phytoplankton community to drastic environmental changes in the Changjiang (Yangtze River) estuary during the past 50 years. Water Res. 54, 1–11. https://doi.org/10.1016/j.watres.2014.01.032.
Keller, G.H., Ye, Y.C., 1985. Geotechnical properties of surface and near-surface deposits in the East China Sea. Cont. Shelf Res. 4, 159–174. https://doi.org/10.1016/0278-4343(85)90027-5.
Klinkhammer, G.P., Bender, M.L., 1981. Trace metal distributions in the Hudson River estuary. Estuar. Coast Shelf Sci. 12, 629–643. https://doi.org/10.1016/S0302-3524(81)80061-8.
Kong, D.X., Miao, C.Y., Borthwick, A.G.L., Duan, Q.Y., Liu, H., Sun, Q.H., Ye, A.Z., Di, Z.H., Gong, W., 2015. Evolution of the Yellow River Delta and its relationship with runoff and sediment load from 1983 to 2011. J. Hydrol. 520, 157–167. https://doi.org/10.1016/j.jhydrol.2014.09.038.
Kuenzer, C., Campbell, I., Roch, M., Leinenkugel, P., Tuan, V.Q., Dech, S., 2013. Understanding the impact of hydropower developments in the context of upstream–downstream relations in the Mekong river basin. Sustain Sci 8, 565–584. https://doi.org/10.1007/s11625-012-0195-z.
Lü, X.X., Song, J.M., Li, X.G., Yuan, H.M., Zhan, T.R., Li, N., Gao, X.L., 2005. Geochemical characteristics of nitrogen in the southern Yellow Sea surface sediments. J. Marine Syst. 56, 17–27. https://doi.org/10.1016/j.jmarsys.2004.06.009.
Lü, Z.Y., Mu, J.X., Liu, S.S., 2017. A review of the impact of climate change and human activities on water environment. China Rural Water Hydropower 65–72. https://doi.org/10.3969/j.issn.1007-2284.2017.02.015.
Li, B., Yan, X.X., He, Z.F., Chen, Y., Zhang, J.H., 2015. Impacts of the three Gorges dam on the bathymetric evolution of the Yangtze River estuary. Chinese Sci. Bull. 60, 1735–1744. https://doi.org/10.1360/N972014-01074.
Li, M.T., Wang, H., Li, Y.M., Ai, W., Hou, L.J., Chen, Z.Y., 2016. Sedimentary BSi and TOC quantifies the degradation of the Changjiang Estuary, China, from river basin alteration and warming SST. Estuar. Coast Shelf Sci. 183, 392–401. https://doi.org/10.1016/j.ecss.2016.08.001.
Li, M.T., Xu, K.Q., Watanabe, M., Chen, Z.Y., 2007. Long-term variations in dissolved silicate, nitrogen, and phosphorus flux from the Yangtze River into the East China Sea and impacts on estuarine ecosystem. Estuar. Coast Shelf Sci. 71, 3–12. https://doi.org/10.1016/j.ecss.2006.08.013.
Lin, S., Huang, K.-M., Chen, S.-K., 2002. Sulfate reduction and iron sulfide mineral formation in the southern East China Sea continental slope sediment. Deep-Sea Res. PT I 49, 1837–1852. https://doi.org/10.1016/S0967-0637(02)00092-4.
Liu, J., Zang, J.Y., Bouwman, L., Liu, S., Yu, Z.G., Ran, X.B., 2016. Distribution and budget of dissolved and biogenic silica in the Bohai sea and Yellow Sea. Biogeochemistry 130, 85–101. https://doi.org/10.1007/s10533-016-0244-2.
Liu, J., Zang, J.Y., Wang, H., Liu, J.H., Bouwman, L., Ran, X.B., 2018. Changes in the distribution and preservation of silica in the Bohai Sea due to changing terrestrial inputs. Cont. Shelf Res. 166, 1–9. https://doi.org/10.1016/j.csr.2018.06.015.
Liu, L.S., Zhou, J., Zheng, B.H., Cai, W.Q., Lin, K.X., Tang, J.L., 2013. Temporal and spatial distribution of red tide outbreaks in the Yangtze River Estuary and adjacent waters, China. Mar. Pollut. Bull. 72, 213–221. https://doi.org/10.1016/j.marpolbul.2013.04.002.
Liu, S.M., Zhang, J., 1998. Normalization of heavy metals to aluminum in marine sediments. Donghai Mar. Sci. 3, 736–741.
Liu, S.M., Zhang, J., Li, D.J., 2004. Phosphorus cycling in sediments of the Bohai and Yellow seas. Estuar. Coast Shelf Sci. 59, 209–218. https://doi.org/10.1016/j.ecss.2003.08.009.
Liu, W., Huang, B., Thorne, P.W., Banzon, V.F., Zhang, H.-M., Freeman, E., Lawrimore, J., Peterson, T.C., Smith, T.M., Woodruff, S.D., 2015. Extended reconstructed sea surface temperature version 4 (ERSST. v4): Part II. Parametric and structural uncertainty estimations. J. Climate 28, 931–951. https://doi.org/10.1175/Jcli-D-14-00007.1.
Luo, X.X., 2012. The Spatial and Temporal Variation in Sediment Grain Size in Middle and Lower Yangtze River, Yangtze Estuary and the Offshore Area Adjacent to Yangtze Estuary - the Impact of Natural Factors and Human Activities. The East China Normal University.
Luo, X.X., Yang, S.L., Zhang, J., 2012. The impact of the Three Gorges Dam on the downstream distribution and texture of sediments along the middle and lower Yangtze River (Changjiang) and its estuary, and subsequent sediment dispersal in the East China Sea. J. Climate 179, 126–140. https://doi.org/10.1016/j.geomorph.2012.05.034.
Müller, B., Berg, M., Yao, Z.P., Zhang, X.F., Wang, D., Pfluger, A., 2008. How polluted is the Yangtze River? Water quality downstream from the three Gorges dam. Sci. Total Environ. 402, 232–247. https://doi.org/10.1016/j.scitotenv.2008.04.049.
Milliman, J.D., 1997. Blessed dams or damned dams? Nature 386, 325. https://doi.org/10.1038/386325a0.
Milliman, J.D., Shen, H.T., Yang, Z.S., Mead, R.H., 1985. Transport and deposition of river sediment in the Changjiang estuary and adjacent continental shelf. Cont. Shelf Res. 4, 37–45. https://doi.org/10.1016/0278-4343(85)90020-2.
Mortlock, R.A., Froelich, P.N., 1989. A simple method for the rapid determination of biogenic opal in pelagic marine sediments. Deep-Sea Res. 36, 1415–1426. https://doi.org/10.1016/0198-0149(89)90092-7.
National Environmental Bureau, 1998. Water and Waste Water Analysis, Thirded. Chinese Environmental Science Publish House, Beijing.
Oehler, T., Martinez, R., Schückel, U., Winter, C., Kröncke, I., Schlüter, M., 2015a. Seasonal and spatial variations of benthic oxygen and nitrogen fluxes in the Helgoland Mud Area (southern North Sea). Cont. Shelf Res. 106, 118–129. https://doi.org/10.1016/j.csr.2015.06.009.
Oehler, T., Schlüter, M., Schückel, U., 2015b. Seasonal dynamics of the biogenic silica cycle in surface sediments of the Helgoland Mud Area (southern North Sea). Cont. Shelf Res. 107, 103–114. https://doi.org/10.1016/j.csr.2015.07.016.
Olli, K., Clarke, A., Danielsson, Å., Aigars, J., Conley, D.J., Tamminen, T., 2008. Diatom stratigraphy and long-term dissolved silica concentrations in the Baltic Sea. J. Marine Syst. 73, 284–299. https://doi.org/10.1016/j.jmarsys.2007.04.009.
Pang, R.S., Pan, S.M., Wang, A.D., 2011. Modern sedimentation rate and its implications for environmental evolutions of the 18# core in the Changjiang Estuary in China. Mar. Sci. Bull. 294-301. https://doi.org/10.3969/j.issn.1001-6392.2011.03.010.
Pilotte, J.O., Winchester, J.W., Glassen, R.C., 1978. Detection of heavy metal pollution in estuarine sediments. Water Air Soil Poll. 9, 363–368. https://doi.org/10.1007/BF00280685.
Presti, M., Michalopoulos, P., 2008. Estimating the contribution of the authigenic mineral component to the long-term reactive silica accumulation on the western shelf of the Mississippi River Delta. Cont. Shelf Res. 28, 823–838. https://doi.org/10.1016/j.csr.2007.12.015.
Ragueneau, O., Leynaert, A., Tréguer, P., Demaster, D.J., Anderson, R.F., 1996. Opal studied as a marker of paleoproductivity. Eos. T Am. Geophys. Un 77, 491-491. https://doi.org/10.1029/96EO00325.
Ran, X.B., Liu, S., Liu, J., Zang, J.Y., Che, H., Ma, Y.X., Wang, Y.B., 2016. Composition and variability in the export of biogenic silica in the Changjiang river and the effect of three Gorges reservoir. Sci. Total Environ. 571, 1191–1199. https://doi.org/10.1016/j.scitotenv.2016.07.125.
Robbins, J.A., Edgington, D.N., 1975. Determination of recent sedimentation rates in Lake Michigan using Pb-210 and Cs-137. Geochim. Cosmochim. AC 39, 285–304. https://doi.org/10.1016/0016-7037(75)90198-2.
Rydin, E., Malmaeus, J.M., Karlsson, O.M., Jonsson, P., 2011. Phosphorus release from coastal Baltic Sea sediments as estimated from sediment profiles. Estuar. Coast Shelf Sci. 92, 111–117. https://doi.org/10.1016/j.ecss.2010.12.020.
Sanchez-Cabeza, J.A., Ruiz-Fernández, A.C., 2012. 210Pb sediment radiochronology: an integrated formulation and classification of dating models. Geochim. Cosmochim. AC 82, 183–200. https://doi.org/10.1016/j.gca.2010.12.024.
Schenau, S.J., De Lange, G.J., 2001. Phosphorus regeneration vs. burial in sediments of the Arabian Sea. Mar. Chem. 75, 201–217. https://doi.org/10.1016/S0304-4203(01)00037-8.
Smith, C.J., DeLaune, R.D., Patrick, W.H., 1985. Fate of riverine nitrate entering an estuary: I. Denitrification and nitrogen burial. Estuaries 8, 15–21. https://doi.org/10.2307/1352117.
Smith, T.M., Reynolds, R.W., Peterson, T.C., Lawrimore, J., 2008. Improvements to NOAA's historical merged land–ocean surface temperature analysis (1880–2006). J. Climate 21, 2283–2296. https://doi.org/10.1175/2007JCLI2100.1.
Sullivan, B.E., Prahl, F.G., Small, L.F., Covert, P.A., 2001. Seasonality of phytoplankton production in the Columbia River: a natural or anthropogenic pattern? Geochim. Cosmochim. AC 65, 1125–1139. https://doi.org/10.1016/S0016-7037(00)

00565-2.
Syvitski, J.P.M., Kettner, A.J., Overeem, I., Hutton, E.W.H., Hannon, M.T., Brakenridge, G.R., Day, J., Vörösmarty, C., Saito, Y., Giosan, L., Nicholls, R.J., 2009. Sinking deltas due to human activities. Nat. Geosci. 2, 681–686. https://doi.org/10.1038/ngeo629.
Syvitski, J.P.M., Vörösmarty, C.J., Kettner, A.J., Green, P., 2005. Impact of humans on the flux of terrestrial sediment to the global coastal ocean. Science 308, 376–380. https://doi.org/10.1126/science.1109454.
Tessler, Z.D., Vörösmarty, C.J., Grossberg, M., Gladkova, I., Aizenman, H., Syvitski, J.P.M., Foufoula-Georgiou, E., 2015. Profiling risk and sustainability in coastal deltas of the world. Science 349, 638–643. https://doi.org/10.1126/science.aab3574.
Thomas, H., Pempkowiak, J., Wulff, F., Nagel, K., 2010. The Baltic Sea: a global synthesis. In: Liu, K.-K., Atkinson, L., Quiñones, R., Talaue-McManus, L. (Eds.), Carbon and Nutrient Fluxes in Continental Margins. Springer, Berlin Heidelberg, pp. 334–345.
Treguer, P., Nelson, D.M., Van Bennekom, A.J., DeMaster, D.J., Leynaert, A., Quéguiner, B., 1995. The silica balance in the world ocean: a reestimate. Science 268, 375–379. https://doi.org/10.1126/science.268.5209.375.
Turner, R.E., Milan, C.S., Rabalais, N.N., 2004. A retrospective analysis of trace metals, C, N and diatom remnants in sediments from the Mississippi River delta shelf. Mar. Pollut. Bull. 49, 548–556. https://doi.org/10.1016/j.marpolbul.2004.03.013.
van der Weijden, A.J., van der Weijden, C.H., 2002. Silica fluxes and opal dissolution rates in the northern Arabian Sea. Deep-Sea Res. PT I 49, 157–173. https://doi.org/10.1016/S0967-0637(01)00050-4.
Walsh, J.J., 2013. On the Nature of Continental Shelves. Elsevier.
Walther, G.-R., Post, E., Convey, P., Menzel, A., Parmesan, C., Beebee, T.J.C., Fromentin, J.-M., Hoegh-Guldberg, O., Bairlein, F., 2002. Ecological responses to recent climate change. Nature 416, 389–395. https://doi.org/10.1038/416389a.
Wang, J.H., Huang, X.Q., Liu, A.C., Zhang, Y.F., 2004. Tendency of the biodiversity variation nearby Changjiang Estuary. Mar. Sci. Bull. 23, 32–39. https://doi.org/10.3969/j.issn.1001-6392.2004.01.006.
Wang, J.H., Wu, J.Y., 2009. Occurrence and potential risks of harmful algal blooms in the East China Sea. Sci. Total Environ. 407, 4012–4021. https://doi.org/10.1016/j.scitotenv.2009.02.040.
Wang, X.D., Yang, S.Y., Ran, X.B., Liu, X.-M., Bataille, C.P., Su, N., 2018. Response of the Changjiang (Yangtze River) water chemistry to the impoundment of three Gorges dam during 2010–2011. Chem. Geol. 487, 1–11. https://doi.org/10.1016/j.chemgeo.2018.04.006.
Windom, H.L., Silpipat, S., Chanpongsang, A., Smith, R.G., Hungspreugs, M., 1984. Trace metal composition of and accumulation rates of sediments in the Upper Gulf of Thailand. Estuar. Coast Shelf Sci. 19, 133–142. https://doi.org/10.1016/0272-7714(84)90060-X.
Winogradow, A., Pempkowiak, J., 2014. Organic carbon burial rates in the Baltic Sea sediments. Estuar. Coast Shelf Sci. 138, 27–36. https://doi.org/10.1016/j.ecss.2013.12.001.
Xu, H., Chen, Z.Y., Finlayson, B., Webber, M., Wu, X.D., Li, M.T., Chen, J., Wei, T.Y., Barnett, J., Wang, M., 2013. Assessing dissolved inorganic nitrogen flux in the Yangtze River, China: sources and scenarios. Global Planet Change 106, 84–89. https://doi.org/10.1016/j.gloplacha.2013.03.005.
Xu, K.H., Milliman, J.D., 2009. Seasonal variations of sediment discharge from the Yangtze River before and after impoundment of the three Gorges dam. Geomorphology 104, 276–283. https://doi.org/10.1016/j.geomorph.2008.09.004.
Xue, Y., Smith, T.M., Reynolds, R.W., 2003. Interdecadal changes of 30-yr SST normals during 1871–2000. J. Climate 16, 1601–1612. https://doi.org/10.1175/1520-0442-16.10.1601.
Yan, W.J., Zhang, S., Wang, J.H., 2001. Nitrogen biogeochemical cycling in the Changjiang Drainage basin and its effect on Changjiang River dissolved inorganic nitrogen: temporal trend for the period 1968~ 1997. J. Geogr. Sci. 56, 505–514. https://doi.org/10.3321/j.issn:0375-5444.2001.05.001.
Yang, H., Xie, P., Ni, L.Y., Flower, R.J., 2012. Pollution in the Yangtze. Science 337, 410-410. https://doi.org/10.1126/science.337.6093.410-a.
Yang, H.F., Yang, S.L., Meng, Y., Xu, K.H., Luo, X.X., Wu, C.S., Shi, B.W., 2018. Recent coarsening of sediments on the southern Yangtze subaqueous delta front: a response to river damming. Cont. Shelf Res. 155, 45–51. https://doi.org/10.1016/j.csr.2018.01.012.
Yang, S.L., Belkin, I.M., Belkina, A.I., Zhao, Q.Y., Zhu, J., Ding, P.X., 2003. Delta response to decline in sediment supply from the Yangtze River: evidence of the recent four decades and expectations for the next half-century. Estuar. Coast Shelf Sci. 57, 689–699. https://doi.org/10.1016/S0272-7714(02)00409-2.
Yang, S.L., Milliman, J.D., Li, P., Xu, K., 2011. 50,000 dams later: erosion of the Yangtze River and its delta. Global Planet Change 75, 14–20. https://doi.org/10.1016/j.gloplacha.2010.09.006.
Yang, Z.S., Chen, X.H., 2007. Centurial high resolution records of sediment grain-size variation in the mud area off the Changjiang(Yangtze River) estuary and its influential factors. Quaternary Sci. 27, 690–699. https://doi.org/10.3321/j.issn:1001-7410.2007.05.010.
Yu, H., Wu, Y., Zhang, J., Deng, B., Zhu, Z.Y., 2011. Impact of extreme drought and the Three Gorges Dam on transport of particulate terrestrial organic carbon in the Changjiang (Yangtze) River. J Geophys Res-Earth 116. https://doi.org/10.1029/2011JF002012.
Yu, L.H., Li, D.J., Fang, T., Li, Y., Gao, L., 2006. Distributions of DSi, DIN and changes of Si: N ratio on summer in Changjiang estuary before and after storage of Three Gorges Reservoir. Acta Ecol. Sin. 26, 2817–2826. https://doi.org/10.3321/j.issn:1000-0933.2006.09.006.
Yu, Y., Song, J.M., Li, X.G., Duan, L.Q., 2012. Geochemical records of decadal variations in terrestrial input and recent anthropogenic eutrophication in the Changjiang Estuary and its adjacent waters. Appl. Geochem. 27, 1556–1566. https://doi.org/10.1016/j.apgeochem.2012.05.002.
Zabel, M., Dahmke, A., Schulz, H.D., 1998. Regional distribution of diffusive phosphate and silicate fluxes through the sediment–water interface: the eastern South Atlantic. Deep-Sea Res PT I 45, 277–300. https://doi.org/10.1016/S0967-0637(97)00073-3.
Zarfl, C., Lumsdon, A.E., Berlekamp, J., Tydecks, L., Tockner, K., 2015. A global boom in hydropower dam construction. Aquat. Sci. 77, 161–170. https://doi.org/10.1007/s00027-014-0377-0.
Zhang, G.X., 2006. History of Population Development in the Yangtze River. Hubei Education press.
Zhang, J., Huang, W.W., Martin, J.M., 1988. Trace metals distribution in Huanghe (Yellow River) estuarine sediments. Estuar. Coast Shelf Sci. 26, 499–516. https://doi.org/10.1016/0272-7714(88)90003-0.
Zhang, J., Zhang, Z.F., Liu, S.M., Wu, Y., Xiong, H., Chen, H.T., 1999. Human impacts on the large world rivers: would the Changjiang (Yangtze River) be an illustration? Global Biogeochem. CY 13, 1099–1105. https://doi.org/10.1029/1999GB900044.
Zhou, M.J., Shen, Z.L., Yu, R.C., 2008. Responses of a coastal phytoplankton community to increased nutrient input from the Changjiang (Yangtze) River. Cont. Shelf Res. 28, 1483–1489. https://doi.org/10.1016/j.csr.2007.02.009.
Zhu, Z.Y., Wu, Y., Zhang, J., Du, J.Z., Zhang, G.S., 2014. Reconstruction of anthropogenic eutrophication in the region off the Changjiang Estuary and central Yellow Sea: from decades to centuries. Cont. Shelf Res. 72, 152–162. https://doi.org/10.1016/j.csr.2013.10.018.
Zhuang, K.L., 2005. Sedimentation Features in the Subaqueous Yangtze Delta. The Ocean University of China.